

Preparation and Characterization of Dimercury(I) Monofluorophosphate(V), Hg₂PO₃F: Crystal Structure, Thermal Behavior, Vibrational Spectra, and Solid-State ³¹P and ¹⁹F NMR Spectra

Matthias Weil,^{*†} Michael Puchberger,[‡] and Enrique J. Baran[§]

Institute for Chemical Technologies and Analytics, Division of Structural Chemistry, Vienna University of Technology, Getreidemarkt 9/164-SC, A-1060 Vienna, Austria, Institute of Materials Chemistry, Vienna University of Technology, Getreidemarkt 9/165-MC, A-1060 Vienna, Austria, and Centro de Química Inorgánica (CEQUINOR/CONICET, UNLP), Facultad de Ciencias Exactas, Universidad Nacional de La Plata, C. Correo 962, 1900-La Plata, Argentina

Received September 8, 2004

Single crystals of anhydrous dimercury(I) monofluorophosphate(V), Hg₂PO₃F (**1**), were obtained by cooling diluted aqueous Hg₂(NO₃)₂ and (NH₄)₂PO₃F solutions from 85 °C to room temperature. Compound **1** crystallizes with eight formula units in the orthorhombic space group *Ibam* (No. 72) and lattice parameters $a = 9.406(2)$ Å, $b = 12.145(3)$ Å, $c = 8.567(2)$ Å. It adopts a new structure type even though a topological relation with dimercury(I) sulfate, Hg₂SO₄, is established. The crystal structure of **1** ($R(F^2) > 2\sigma(F^2) = 0.0353$) exhibits Hg₂²⁺ dumbbells and discrete PO₃F²⁻ anions as single building units which are organized in a layered assembly parallel to (100). The symmetric Hg₂²⁺ dumbbell shows a typical Hg–Hg distance of 2.5051(9) Å, and for each Hg atom, three Hg–O distances are found, ranging from 2.327(6) to 2.476(5) Å. No interactions between Hg and F atoms are realized. The latter is exclusively bonded to the phosphorus atom at a distance $d(\text{P–F}) = 1.568(8)$ Å which is considerably longer than the P–O distances with a mean of 1.515 Å. Compound **1** was further characterized by vibrational spectroscopy (Raman and IR) in the spectral range between 4000 and 50 cm⁻¹, thermal analysis (TG, DSC) up to 650 °C which revealed Hg₂(P₂O₇) and Hg₃(PO₄)₂ as thermal decomposition products, and ¹⁹F and ³¹P solid-state NMR spectroscopy. The value for the P–F coupling constant in **1** is $J_{\text{PF}} = -1072$ Hz at 20 °C. The absolute sign of J_{PF} is negative.

Introduction

The crystal chemistry of mercury oxo compounds, and in particular of mercury(I) with its characteristic Hg₂²⁺ dumbbell, is more or less singular. For current reviews of this structural family, see, for instance, refs 1–4. Most of the known mercurous compounds crystallize in unique structure

types without any relation to other phases with monovalent cations and the same anions; for example, Hg₂SeO₄⁵ and Na₂SeO₄⁶ adopt completely different structures. In recent years, the preparation and structural characterization of mercury(I) oxo compounds has therefore attracted much attention, even with regards to theoretical calculations of the geometry of the Hg₂²⁺ dumbbell and the surrounding oxygen atoms, or the prediction of [Hg–Hg–O] units in various crystal structures.⁷

The present project was started to investigate the peculiarities and structural changes caused by a replacement of oxygen by fluorine in tetrahedral XO₄ groups with monovalent mercury as cationic component. A suitable candidate for this purpose was anhydrous dimercury(I) monofluoro-

* To whom correspondence should be addressed. E-mail: mweil@mail.zserv.tuwien.ac.at. Phone: ++43-1-58801-17122. Fax: ++43-1-58801-17199.

† Institute for Chemical Technologies and Analytics, Division of Structural Chemistry, Vienna University of Technology.

‡ Institute of Materials Chemistry, Vienna University of Technology.

§ Universidad Nacional de La Plata.

- (1) Pervukhina, N. V.; Magarill, S. A.; Borisov, S. V.; Romanenko, G. V.; Pal'chik, N. A. *Russ. Chem. Rev.* **1999**, *68*, 615–636.
- (2) Borisov, S. V.; Magarill, S. A.; Romanenko, G. V.; Pervukhina, N. V. *J. Struct. Chem.* **2000**, *41*, 272–279.
- (3) Borisov, S. V.; Magarill, S. A.; Pervukhina, N. V.; Kryuchova, N. A. *J. Struct. Chem.* **2002**, *43*, 293–303.
- (4) Bretinger, D. K. Cadmium and mercury. In *Comprehensive Coordination Chemistry II*; McCleverty, J. A., Meyer, T. J., Eds.; Elsevier: Oxford, 2004; Vol. 6, pp 1253–1292.

(5) Dorm, E. *Acta Chem. Scand.* **1969**, *23*, 1607–1615.

(6) Mehrotra, B. N.; Hahn, T.; Eysel, W.; Röpke, H.; Illguth, A. *Neues Jahrb. Mineral., Monatsh.* **1978**, 408–421.

(7) Wang, S. G.; Qiu, Y. X.; Neumann, E.; Deiseroth, H. J.; Schwarz, W. H. E. *Z. Anorg. Allg. Chem.* **2003**, *629*, 1718–1730.

phosphate(V),⁸ Hg₂PO₃F, which has been known for nearly 80 years,¹² but which has since not been structurally characterized. Fluorophosphoric acid and sulfuric acid are isoelectronic, and due to the closely related configuration of the tetrahedral PO₃F²⁻ and SO₄²⁻ anions, one might expect similar physical and chemical properties for the corresponding compounds with the same cation, in this case Hg₂PO₃F and Hg₂SO₄. Indeed, some monofluorophosphates and sulfates crystallize in the same structure type, viz. Na₂PO₃F·10H₂O¹³ and Na₂SO₄·10H₂O,¹⁴ β-K₂PO₃F¹⁵ and β-K₂SO₄,¹⁶ or BaPO₃F¹⁷ and BaSO₄,¹⁸ although no structure refinement was performed for BaPO₃F.

In this Article, the preparation and characterization of Hg₂-PO₃F with single crystal X-ray diffraction, thermal analysis, vibrational spectroscopy, and solid-state NMR spectroscopy are reported, and a comparative structural description of Hg₂-PO₃F and Hg₂SO₄ is given.

Experimental Section

Preparation. All reagents used were of analytical grade. Polycrystalline (NH₄)₂PO₃F was synthesized according to ref 19 from stoichiometric mixtures of (NH₄)₂HPO₄ and NH₄F·HF in a urea melt at 170 °C for 2 h. The obtained product was then recrystallized from an acetone/water solution. XRPD revealed a single phase product.

The following procedure for the preparation of microcrystalline Hg₂PO₃F was carried out at room temperature. Under constant stirring, a 2 × 10⁻³ M (NH₄)₂PO₃F solution was slowly added to a slightly acidified 10⁻³ M Hg₂(NO₃)₂ solution. Close to the area where the monofluorophosphate solution was dropped in, a light-yellow solid precipitated that immediately dissolved under further stirring. When the saturation point was exceeded, visible by a colorless clouding of the solution, further addition of the monofluorophosphate solution was stopped, and a few drops of half-concentrated nitric acid were added. The solution became clear again and was then filtered and placed in a crystallizing dish. Very small colorless Hg₂PO₃F crystals formed overnight.

Larger Hg₂PO₃F crystals suitable for conventional X-ray structure analysis were grown using a slightly modified procedure. A hot (ca. 85 °C) diluted Hg₂(NO₃)₂ solution was added quickly to the ammonium monofluorophosphate solution, and the resulting solution was slowly cooled to room temperature. After 1 day,

Table 1. Details of Data Collection, Structure Solution, and Refinement for **I**

radiation, wavelength λ [Å]	Mo Kα, 0.71073
collection temp [°C]	22(2)
fw [g·mol ⁻¹]	499.15
space group, no.	<i>Ib</i> am, No. 72
cryst dimensions [mm ³]	0.35 × 0.05 × 0.02
cryst description	colorless bar
formula units Z	8
a [Å]	9.406(2)
b [Å]	12.145(3)
c [Å]	8.567(2)
V [Å ³]	978.7(4)
μ [mm ⁻¹]	62.910
X-ray density [g·cm ⁻³]	6.776
range θ _{min} –θ _{max}	2.74–30.51
range h, k, l	–13 ≤ h ≤ 13, –17 ≤ k ≤ 16, –12 ≤ l ≤ 12
measured reflns	5400
indep reflns	795
obsd reflns [I > 2σ(I)]	678
R _i	0.0644
coeff trans T _{min} ; T _{max}	0.0620; 0.2711
no. params	38
extinction coeff (SHELXL97)	0.00019(5)
difference electron	Δρ _{max} = 3.255; [0.70, Hg]
density [e·Å ⁻³] with	Δρ _{min} = –2.995; [0.69, Hg]
distance to atom [Å]	
R[F ² > 2σ(F ²); wR(F ² all)]	0.0353; 0.0879
GO F	1.068
CSD number	414292

interpenetrating colorless crystals with a lathlike habit and up to 5 mm in length had formed. It is notable that the latter preparation method frequently yields large single crystals of (Hg₂)₂(PO₄)NO₃·H₂O²⁰ and/or single crystals of β-(Hg₂)₃(PO₄)₂²¹ as main reaction products. This is caused by the hydrolysis of the monofluorophosphate anion which considerably increases with temperature.¹²

Single Crystal Diffraction Intensities were collected in the ω-scan technique with 0.3° rotation width and 30 s exposure time per frame using a SMART three-circle diffractometer (Siemens) equipped with an APEX CCD camera. Three independent sets of 600 frames were recorded thus scanning the whole reciprocal sphere. The measured intensities were corrected for Lorentz and polarization effects, and due to the high linear absorption coefficient an absorption correction was applied using the program HABITUS.²² The crystal structure of Hg₂PO₃F was solved by direct methods and refined with the SHELXL97 program package.²³ In the final refinement cycles, the thermal parameters of all atoms were refined with anisotropic displacement parameters, and the final difference Fourier maps did not indicate any additional atomic sites. The highest difference peaks were located close to the mercury positions. Crystal data of this new compound were standardized with the program STRUCTURE-TIDY.²⁴ Further details of the data collection and refinement are summarized in Table 1, atomic parameters and isotropic displacement parameters are given in Table 2, and selected distances and angles as well as bond-valence sums (BVS) for the individual atoms are listed in Table 3. Drawings of structural details were produced using the program ATOMS.²⁵

- (8) It should be noted that there is some confusion about the term “fluorophosphate” in the literature. It is correct to describe compounds with this notation where one or more O atoms of the PO₄³⁻ tetrahedron are replaced by the corresponding numbers of F atoms (“monofluorophosphate”, PO₃F²⁻; “difluorophosphate”, PO₂F₂⁻). However, this nomenclature should not be used for compounds where distinct PO₄³⁻ tetrahedra and additional F atoms are present in the structure as was done for compounds with general formula M₂(PO₄)F (M = Cu, Cd, Mn).^{9–11} These compounds are better described as phosphate fluorides.
- (9) Rea, J. R.; Kostiner, E. *Acta Crystallogr.* **1976**, *B32*, 1944–1947.
- (10) Rea, J. R.; Kostiner, E. *Acta Crystallogr.* **1974**, *B30*, 2901–2903.
- (11) Rea, J. R.; Kostiner, E. *Acta Crystallogr.* **1972**, *B28*, 2525–2529.
- (12) Lange, W. *Ber. Dtsch. Chem. Ges.* **1929**, *62B*, 793–801.
- (13) Prescott, H. A.; Troyanov, S. I.; Kemnitz, E. *J. Solid State Chem.* **2001**, *156*, 415–421.
- (14) Levy, A. H.; Lisensky, G. C. *Acta Crystallogr.* **1978**, *B34*, 3502–3510.
- (15) Payen, J. L.; Durand, J.; Cot, L.; Galigné, J.-L. *Can. J. Chem.* **1979**, *57*, 886–889.
- (16) McGinney, J. A. *Acta Crystallogr.* **1972**, *B28*, 2845–2852.
- (17) Bengtsson, E. *Ark. Kemi., Mineral. Geol.* **1941**, *15b*, 8.
- (18) Hill, R. J. *Can. Mineral.* **1977**, *15*, 522–526.
- (19) Schülke, U.; Kayser, R. Z. *Anorg. Allg. Chem.* **1991**, *600*, 221–226.

- (20) Durif, A.; Tordjman, I.; Masse, R.; Guitel, J. C. *J. Solid State Chem.* **1978**, *24*, 101–105.
- (21) Weil, M.; Glaum, R. *Z. Anorg. Allg. Chem.* **1999**, *625*, 1752–1761.
- (22) Herrendorf, W. *HABITUS. Programm zur Optimierung der Kristallgestalt anhand geeigneter ψ-abgetasteter Reflexe*; Universities of Karlsruhe and Giessen: Germany, 1993–1997.
- (23) Sheldrick, G. M. *SHELXL97. Programs for crystal structure solution and refinement*; University of Göttingen: Göttingen, Germany, 1997.
- (24) Gelato, L. M.; Parthé, E. *J. Appl. Crystallogr.* **1987**, *20*, 139–143.
- (25) Dowty, E. *ATOMS for Windows*, Version 5.1; Shape Software: Kingsport, TN, 2001.

Table 2. Atomic Coordinates and Equivalent Isotropic Displacement Parameters [\AA^2] for $\text{Hg}_2\text{PO}_3\text{F}$

atom	Wyckoff position	x	y	z	U_{eq}^a
Hg	16k	0.20348(5)	0.10146(3)	0.22378(5)	0.0376(2)
P	8j	0.4532(3)	0.2398(2)	0	0.0174(5)
F	8j	0.0358(9)	0.3724(7)	0	0.0375(18)
O1	16k	0.3643(6)	0.2368(5)	0.1479(7)	0.0255(12)
O2	8j	0.0614(9)	0.1687(8)	0	0.0265(18)

$$^a U_{\text{eq}} = (1/3) \sum_i U_{ii} a_i^* a_i$$

Table 3. Selected Interatomic Distances [\AA], Angles [deg], and Bond Valence Sums (BVS) [v.u.]^a

Hg–O1	2.327(6)	O1–Hg–Hg#2	138.18(15)
Hg–O1#1	2.339(6)	O1#1–Hg–Hg#2	137.87(14)
Hg–O2	2.476(5)	O2–Hg–Hg#2	117.6(2)
Hg–Hg#2	2.5051(9)		
P–O2#3	1.507(9)	O2#3–P–O1#4	112.9(3)
P–O1	1.519(6)	O2#3–P–O1	112.9(3)
P–O1#4	1.519(6)	O1#4–P–O1	113.1(5)
P–F#3	1.568(8)	O2#3–P–F#3	107.9(5)
		O1#4–P–F#3	104.6(3)
		O1–P–F#3	104.6(3)

^a Symmetry transformations used to generate equivalent atoms: #1 $-x + 1/2, -y + 1/2, -z + 1/2$; #2 $x, -y, -z + 1/2$; #3 $x + 1/2, -y + 1/2, z$; #4 $x, y, -z$. BVS: Hg 1.11, P 5.10, F 1.15, O1 1.89, O2 1.75.

Vibrational Spectra. The infrared spectra in the spectral range between 4000 and 300 cm^{-1} were recorded as KBr pellets with a Bruker IFS 66 FTIR instrument. A total of 60 scans were accumulated. Spectral resolution was $\pm 4 \text{ cm}^{-1}$. Raman spectra in the spectral range between 1500 and 50 cm^{-1} were obtained with the FRA 106 Raman accessory of the mentioned spectrophotometer. The samples were excited with the 1064 nm line of a solid-state Nd:YAG laser.

Thermal Analysis. Thermoanalytical measurements (TG, DSC) were performed in an open system under a flowing N_2 atmosphere (200 mL/min) and a heating rate of 5 $^\circ\text{C}/\text{min}$ on a Mettler-Toledo TG-50 system (35–650 $^\circ\text{C}$, corundum crucibles) and a Mettler-Toledo DSC-25 system (35–500 $^\circ\text{C}$, aluminum capsules). The intermediate and remaining microcrystalline solids obtained after the heating cycles were identified by subsequent X-ray powder diffraction.

NMR Spectra. The ^{19}F and ^{31}P solid-state NMR spectra were measured at room temperature on a Bruker AVANCE 300 spectrometer using a 4 mm MAS broadband probe head. The spinning frequency was 12 kHz. The ^{19}F resonance frequency was 282.14 MHz, and the ^{31}P resonance frequency was 121.38 MHz. The external references for the isotropic chemical shift determination were against C_6F_6 (^{19}F : 164.9 ppm) and phosphoric acid, H_3PO_4 (^{31}P : 0 ppm).

Results and Discussion

Structure Description. Under the given experimental conditions, a possible hydrolysis of the monofluorophosphate ion resulting in a replacement of F by OH^- ions has to be considered. However, IR measurements of bulk material in the range 4200–2000 cm^{-1} did not reveal any incorporation of OH into the structure.

$\text{Hg}_2\text{PO}_3\text{F}$ is not isotopic with the corresponding sulfate Hg_2SO_4 (monoclinic, $P2_1/c$, $Z = 2$, $a = 6.2802(9) \text{ \AA}$, $b = 4.4273(5) \text{ \AA}$, $c = 8.367(2) \text{ \AA}$, $\beta = 91.76^\circ$)⁵ and crystallizes in a new structure type, even though both compounds show some topological relations which are illustrated in Figure 1.

The crystal structure of $\text{Hg}_2\text{PO}_3\text{F}$ consists of Hg_2^{2+} dumbbells and discrete PO_3F^{2-} anions as the main building units which are organized in a layered assembly. The Hg_2^{2+} dumbbells share O atoms and form layers parallel to (100). The P atoms are situated between and connect the layers perpendicularly via common O atoms along the [100] direction. The P atom is also bonded to one F atom which shows no bonding interaction to the metal centers since the shortest Hg–F distance is 3.423(6) \AA . A similar arrangement is realized in Hg_2SO_4 which is made up of Hg_2^{2+} dumbbells and SO_4^{2-} anions as main building units. Here, the Hg_2^{2+} dumbbells also share O atoms with each other and form layers parallel to (001). These layers are linked by S atoms along [001].

In both compounds, the Hg–Hg distances of 2.5051(9) \AA ($\text{Hg}_2\text{PO}_3\text{F}$) and of 2.500(3) \AA (Hg_2SO_4) are nearly the same and are very close to the mean of 2.518(± 25) \AA calculated for nearly 100 different Hg_2^{2+} dumbbells observed in various other Hg(I) oxo compounds. In the title compound, the Hg_2^{2+} dumbbell has a symmetric oxygen environment (Figure 2) with three O atoms in the coordination sphere for each Hg atom, if a bonding interaction between Hg and the surrounding atoms is considered for distances $< 3.0 \text{ \AA}$. The Hg–O distances range from 2.327(6) to 2.476(5) \AA . In Hg_2SO_4 , the Hg_2^{2+} dumbbell is surrounded by four O atoms with Hg–O distances in the range from 2.23 to 2.93 \AA . Unlike other Hg(I) compounds which frequently show a more or less linear $\angle(\text{Hg}-\text{Hg}-\text{X})$ angle between the dumbbell and the tightly bonded X atom ($\text{X} = \text{O}, \text{S}, \text{Se}, \text{Hal}$), in $\text{Hg}_2\text{PO}_3\text{F}$ all $\angle(\text{Hg}-\text{Hg}-\text{O})$ angles are bent with values ranging from 117.6(2) $^\circ$ to 138.18(15) $^\circ$. The slightly distorted PO_3F tetrahedron shows point symmetry $\dots m$ and has three very similar P–O distances with a mean of 1.515 \AA and one considerably longer P–F distance of 1.568(8) \AA . The elongation of the P–F bond length with respect to the P–O bond distances is characteristic for the PO_3F tetrahedron and is also observed in other anhydrous monofluorophosphates, for example, in $\beta\text{-Na}_2\text{PO}_3\text{F}$,²⁶ $\bar{d}(\text{P}-\text{O}) = 1.493 \text{ \AA}$, $\bar{d}(\text{P}-\text{F}) = 1.606 \text{ \AA}$, and in SnPO_3F ,²⁷ $\bar{d}(\text{P}-\text{O}) = 1.48 \text{ \AA}$, $d(\text{P}-\text{F}) = 1.57 \text{ \AA}$. The shortest interpolyhedral F–F distance in $\text{Hg}_2\text{PO}_3\text{F}$ is 3.171(18) \AA .

Both O1 and O2 are bonded to two Hg atoms and one P atom resulting in a considerable distorted trigonal coordination figure around each of the central oxygen atoms.

The results of the bond-valence calculations,²⁸ using the parameters of Brese and O'Keeffe,²⁹ are in accordance with the expected formal charges (see Table 3).

Thermal Behavior. Decomposition of the material starts with onset of ca. 285 $^\circ\text{C}$ (Figure 3). Qualitative phase analysis of the remaining solid obtained at 330 $^\circ\text{C}$ revealed $\text{Hg}_2\text{PO}_3\text{F}$ as the main phase and mercury(I) diphosphate, $(\text{Hg}_2)_2(\text{P}_2\text{O}_7)$,³⁰ as a secondary product (eq 1a). At 370 $^\circ\text{C}$, no more $\text{Hg}_2\text{PO}_3\text{F}$ was identified by XRPD, but $(\text{Hg}_2)_2(\text{P}_2\text{O}_7)$

(26) Durand, J.; Cot, L.; Galigné, J.-L. *Acta Crystallogr.* **1974**, *B30*, 1565–1569.

(27) Berndt, A. F. *Acta Crystallogr.* **1974**, *B30*, 529–530.

(28) Brown, I. D. *The Chemical Bond in Inorganic Chemistry*; Oxford University Press: Oxford, 2002.

(29) Brese, N. E.; O'Keeffe, M. *Acta Crystallogr.* **1991**, *B47*, 192–197.

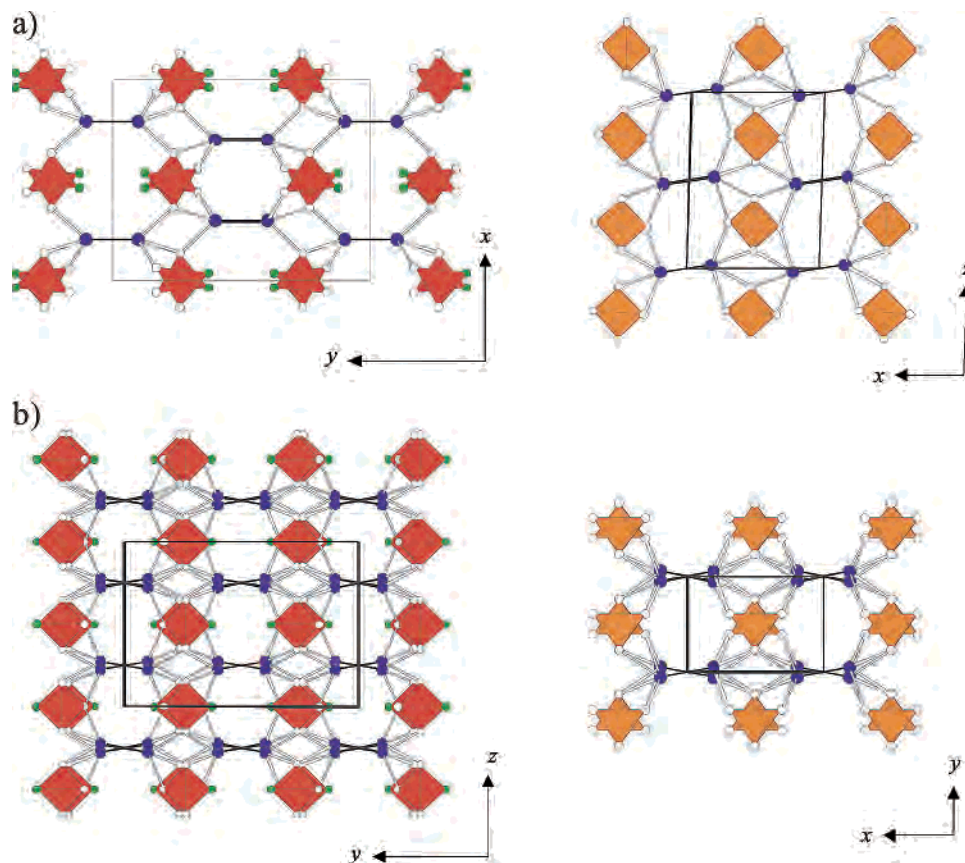


Figure 1. Crystal structures of $\text{Hg}_2\text{PO}_3\text{F}$ (left) and Hg_2SO_4 (right) in polyhedral representation with projections down [001] (a) and [100] (b) for $\text{Hg}_2\text{PO}_3\text{F}$, and [010] (a) and [001] (b) for Hg_2SO_4 . The Hg atoms are given as blue spheres, F atoms as green spheres, and O atoms as white spheres; PO_3F tetrahedra are red, and SO_4 tetrahedra are orange.

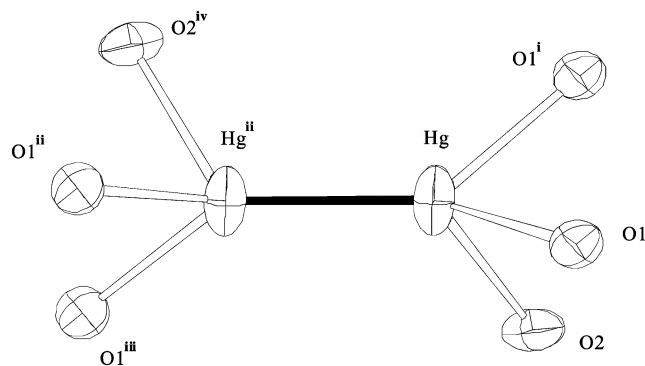


Figure 2. Oxygen environment around the Hg_2^{2+} dumbbell with displacement ellipsoids drawn at the 74% probability level. Symmetry codes: (i) $-x + 1/2, -y + 1/2, -z + 1/2$; (ii) $x, -y, -z + 1/2$; (iii) $-x + 1/2, -y - 1/2, -z$; (iv) $x, -y, z + 1/2$.

(main phase) and mercury(II) orthophosphate, $\text{Hg}_3(\text{PO}_4)_2$,³¹ (secondary phase) were identified instead (eq 1a,b). Above 400 °C, only $\text{Hg}_3(\text{PO}_4)_2$ and mercury(II) diphosphate, $\text{Hg}_2(\text{P}_2\text{O}_7)$,³² in an estimated ratio of about 1:2, were found (eq 1b,c). These observations support a proposed three-step mechanism whereby only two endothermic effects at ca. 330 and 380 °C, respectively, are clearly visible in the corresponding DSC measurement. The decomposition range of the intermediately formed $(\text{Hg}_2)_2(\text{P}_2\text{O}_7)$ is in agreement with

(30) Weil, M.; Glaum, R. *Z. Anorg. Allg. Chem.* **1999**, 625, 1752–1761.
 (31) Aurivillius, K.; Nilsson, B. A. *Z. Kristallogr.* **1975**, 141, 1–10.
 (32) Weil, M.; Glaum, R. *Acta Crystallogr.* **1997**, C53, 1000–1003.

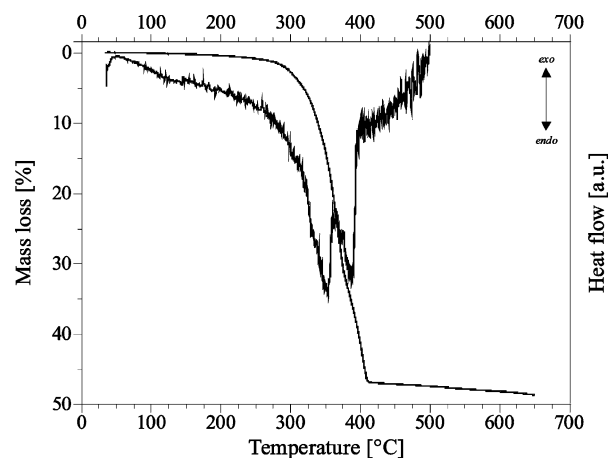
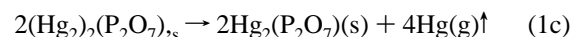
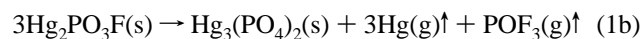
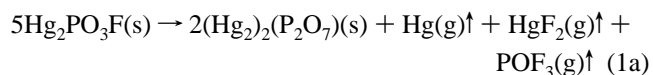


Figure 3. $\text{Hg}_2\text{PO}_3\text{F}$. TG and DSC plot of the thermal treatment between 35 and 650 °C.

the thermal behavior³⁰ of single phase $(\text{Hg}_2)_2(\text{P}_2\text{O}_7)$ which decomposes between 300 and 400 °C under release of mercury into $\text{Hg}_2(\text{P}_2\text{O}_7)$ (eq 1c).

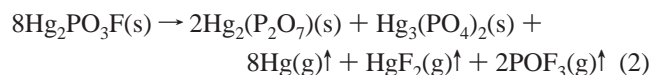


The theoretical mass loss calculated with respect to the idealized overall reaction (eq 2) is in good agreement with

Table 4. Unit Cell Group Analysis of the PO_3F^{2-} Vibrations in the $\text{Hg}_2\text{PO}_3\text{F}$ Lattice (Space Group D_{2h} ;³⁶ $Z = 8/2$)

	“free” anion	site symmetry	factor group
	C_{3v}	C_s	D_{2h}
$\nu_1 \nu(\text{P-F})$	A_1	A'	$A_{1g} + B_{2g} + B_{1u} + B_{3u}$
$\nu_2 \nu_s(\text{PO}_3)$	A_1	A'	$A_{1g} + B_{2g} + B_{1u} + B_{3u}$
$\nu_3 \delta(\text{FPO}_3)$	A_1	A'	$A_{1g} + B_{2g} + B_{1u} + B_{3u}$
$\nu_4 \nu_{as}(\text{PO}_3)$	E	$A' + A''$	$A_{1g} + B_{2g} + B_{1u} + B_{3u} + B_{1g} + B_{3g} + A_u + B_{2u}$
$\nu_5 \delta(\text{PO}_3)$	E	$A' + A''$	$A_{1g} + B_{2g} + B_{1u} + B_{3u} + B_{1g} + B_{3g} + A_u + B_{2u}$
$\nu_6 \rho(\text{PO}_3)$	E	$A' + A''$	$A_{1g} + B_{2g} + B_{1u} + B_{3u} + B_{1g} + B_{3g} + A_u + B_{2u}$
activity A_1, E :	IR, Raman	A', A'' : IR, Raman	$A_{1g}, B_{1g}, B_{2g}, B_{3g}$: Raman B_{1u}, B_{2u}, B_{3u} : IR A_u : inactive

the experimental value (theoretical mass loss 48.6%, observed 47.2%):



Vibrational Spectra. On the basis of the reported structural data, it is possible to attempt an analysis of the vibrational spectra, performing a factor group analysis of the investigated lattice, correlating the symmetry of the “free” PO_3F^{2-} anion, its site symmetry, and its unit cell factor group.^{33–35} This analysis is shown in Table 4. As it can be seen, under site symmetry conditions the double degenerated E modes are split, and all vibrations remain IR and Raman active, whereas under unit cell group symmetry a greater number of bands is predicted. In this last case, the exclusion principle becomes operative, and IR and Raman active modes belong to phonons of different parity.

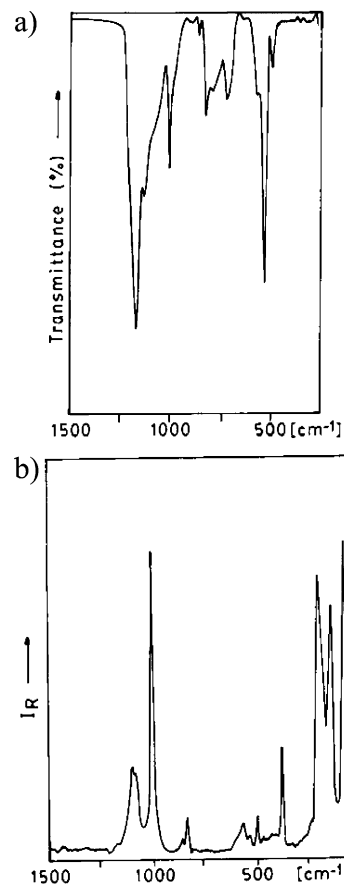
The measured infrared and Raman spectra of the compound are shown in Figure 4. The weak splitting of some of the bands suggests that the spectrum should be interpreted on the basis of the unit cell group symmetry. The proposed assignment is presented in Table 5 and is briefly commented on, as follows: (i) The $\nu(\text{P-F})$ vibration lies at a slightly higher frequency than the solution value measured by Raman spectroscopy (795 cm^{-1}).³⁶ This vibration is split in both spectra, but the weaker component lies at a higher frequency than the main band in the Raman spectrum whereas the inverse situation is observed in the IR spectrum. (ii) The two $\nu(\text{PO}_3)$ vibrations are also split in both spectra. As commented above for the $\nu(\text{P-F})$ vibration, the same intensity inversion is observed for the $\nu_s(\text{PO}_3)$ vibration; in contrast, in the $\nu_{as}(\text{PO}_3)$ band the weaker component is seen at lower energy in both spectra. (iii) In the solution Raman spectrum, the ν_3 and ν_5 bands are found at the same energy (520 cm^{-1}).³⁶ In the present crystal spectra, we have assigned $\nu_5 > \nu_3$, on the basis of intensity criteria, as the ν_5 vibration must be of higher intensity in the IR spectrum, as observed.

(33) Ross, S. D. *Inorganic Infrared and Raman Spectra*; McGraw-Hill: London, 1972.

(34) Müller, A.; Baran, E. J.; Carter, R. O. *Struct. Bonding* **1976**, *26*, 81–139.

(35) Fadini, A.; Schnepel, F. M. *Vibrational Spectroscopy. Methods and Applications*; Ellis Horwood: Chichester, U.K., 1989.

(36) Siebert, H. *Anwendungen der Schwingungsspektroskopie in der Anorganischen Chemie*; Springer-Verlag: Berlin, 1966.

**Figure 4.** $\text{Hg}_2\text{PO}_3\text{F}$. (a) FTIR spectrum in the spectral range between 1500 and 300 cm^{-1} and (b) Raman spectrum in the spectral range between 1500 and 50 cm^{-1} .**Table 5.** Assignment of the IR and Raman Spectra of $\text{Hg}_2\text{PO}_3\text{F}$ (Band Positions in cm^{-1})^a

IR	Raman	assignment
1166 vs, 1125 vw	1098 s, 1081 sh	$\nu_4, \nu_{as}(\text{PO}_3)$
1006 s, 985 sh	1003 vs	$\nu_2, \nu_s(\text{PO}_3)$
824 m, 781 w	880 w, 837 m	$\nu_1, \nu(\text{P-F})$
568 w, 534 vs	566 m, 536 w	$\nu_5, \delta(\text{PO}_3)$
491 w	496 m	$\nu_3, \delta(\text{FPO}_3)$
360 vw (?)	375 s	$\nu_6, \rho(\text{PO}_3)$
	199 vs	$\nu(\text{Hg-Hg})$
	137 vs, 87 vs	lattice modes

^a vs, very strong; s, strong; m, medium; w, weak; vw, very weak; sh, shoulder.

This $\delta(\text{PO}_3)$ vibration appears split in both spectra, also with an inversion of the relative position of the weaker component. (iv) The rocking mode, ν_6 , found at 379 cm^{-1} in the solution spectrum,³⁶ is seen as a strong Raman line at 375 cm^{-1} whereas it is only observed as a very weak IR feature. (v) Only one of the four expected unit cell group Hg–Hg vibrations could be identified with certainty. It is the very strong Raman line at 199 cm^{-1} , which was assigned by comparison with values reported in $\text{Hg}_2(\text{NO}_3)_2$ solution³⁶ and in other formerly investigated Hg(I) compounds.^{37,38} (vi) The last two Raman lines (137 and 87 cm^{-1}) are surely related to external (lattice) vibrations of the crystalline solid.

(37) Baran, E. J.; Schriewer-Pöttgen, M. S.; Jeitschko, W. *Spectrochim. Acta* **1996**, *A52*, 441–444.

(38) Baran, E. J.; Mormann, T.; Jeitschko, W. *J. Raman Spectrosc.* **1999**, *30*, 1049–1051.

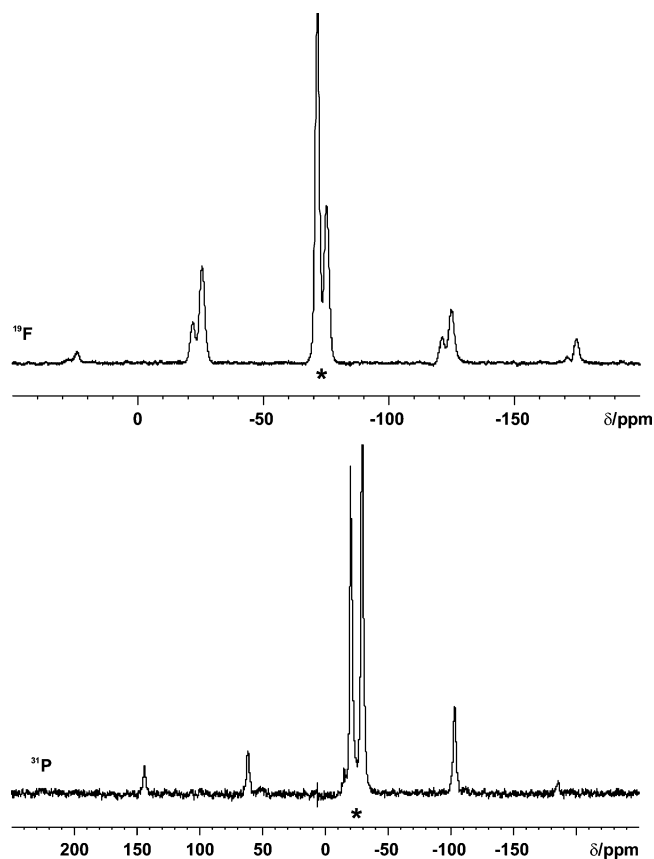


Figure 5. Experimental ^{31}P and ^{19}F solid-state NMR spectra of $\text{Hg}_2\text{PO}_3\text{F}$. MAS centerbands have been labeled with an asterisk. All other bands are MAS rotation sidebands.

As can be seen in Table 5, most of the corresponding IR and Raman bands show different frequency values in agreement with their different phononic origins (cf. Table 4). These differences are usually considered as a valuable criterion for the evaluation of the strength of coupling effects in the unit cell^{39,40} and confirm that these effects are relatively important in the present lattice.

Finally, it should be commented that the medium intensity IR band located at 705 cm^{-1} is not related to $\text{Hg}_2\text{PO}_3\text{F}$. It is an impurity, probably originating from slow decomposition of the compound, after storage.

NMR Spectra. The solid-state ^{19}F and ^{31}P NMR spectra are consistent with the structural data. The ^{31}P signal appears

(39) Müller, A. *Z. Naturforsch.* **1966**, *21a*, 433–436.

(40) Baran, E. J.; Ferrer, E. G.; Bueno, I.; Parada, C. *J. Raman Spectr.* **1990**, *21*, 27–30.

at -25.0 ppm as a doublet with a scalar spin–spin coupling constant of $J_{\text{PF}} = -1072\text{ Hz}$. The ^{19}F signal appears at -73.6 ppm as a doublet and shows the same coupling constant as the ^{31}P signal (Figure 5). The absolute sign of J_{PF} is negative. The obtained value and the absolute sign for J_{PF} are in agreement with previous solid-state and solution NMR studies of other monofluorophosphates.^{41–46} Their coupling constants are of the same negative sign and have magnitudes in the range $500\text{--}1500\text{ Hz}$.

Summary

Anhydrous dimercury(I) monofluorophosphate(V), $\text{Hg}_2\text{PO}_3\text{F}$ (**1**), was prepared from diluted aqueous solutions of $(\text{NH}_4)_2\text{PO}_3\text{F}$ and $\text{Hg}_2(\text{NO}_3)_2$. The crystal structure is made up of Hg_2^{2+} units and PO_3F^{2-} tetrahedra as simple building units which are organized in a layered assembly parallel to (100). The F atom shows no interaction with the Hg_2^{2+} dumbbell and is exclusively bonded to the P atom. Upon heating above 400 °C , **1** converts to a mixture of $\text{Hg}_3(\text{PO}_4)_2$ and $\text{Hg}_2(\text{P}_2\text{O}_7)$. The vibrational spectra (IR, Raman) were interpreted by means of a unit cell group analysis. The results of solid-state ^{31}P and ^{19}F NMR spectroscopic measurements are consistent with the structure data and revealed a P–F coupling constant of $J_{\text{PF}} = -1072\text{ Hz}$. In agreement with other monofluorophosphates, the absolute sign of J_{PF} is negative.

Acknowledgment. Part of this work was supported by CONICET (Argentina). E.J.B. is a member of the Research Career of this organization.

Supporting Information Available: Crystallographic information file (CIF) for the structure reported herein, which is also available through the Fachinformationszentrum Karlsruhe, D-76344 Eggenstein-Leopoldshafen (crysdata@FIZ-Karlsruhe.de), on quoting this article and the deposition number listed at the end of Table 1. This material is available free of charge via the Internet at <http://pubs.acs.org>.

IC048741E

(41) VanderHart, D. L.; Gutowsky, H. S.; Farrar, T. C. *J. Chem. Phys.* **1969**, *50*, 1058–1065.

(42) Grimmer, A. R.; Müller, D.; Neels, J. Z. *Chem.* **1983**, *23*, 140–142.

(43) Grimmer, A. R.; Jost, K. H.; Müller, D.; Neels, J. *J. Fluorine Chem.* **1987**, *34*, 347–360.

(44) Farrar, T. C.; Jablonsky, M. J. *J. Phys. Chem.* **1991**, *95*, 9159–9166.

(45) Farrar, T. C.; Trudeau, J. D. *NATO ASI Ser., Ser. C* **1993**, *C386*, 27–48.

(46) Farrar, T. C.; Schwartz, J. L.; Rodríguez, S. *J. Phys. Chem.* **1993**, *97*, 7201–7207.